

Numerical Study of Reinforced Concrete Columns by Using Steel Slag and Reinforced by Fiber Polymer Glass Bars

Qais M. Aljabri¹, Ehab M. lofty², Manar A.³, Ibrahim H. El-kersh⁴

¹Civil Engineering Department, Faculty of Engineering, Thamar University, Yemen

^{2,3,4}Civil Engineering Department, Faculty of Engineering, Suez Canal University, Egypt

Abstract- Worldwide relevancy in reinforced concrete (RC) technology for the last 100 years have shown that RC structures show a dependable and lasting behavior when they are suitably designed, constructed and maintained. However, porosity and cracking of concrete, as well as corrosion of steel reinforcement can induce to failure of existing RC structures particularly when they are exposed to greatest and antagonistic environmental requisite and extreme loads. Glass fiber reinforced polymer (GFRP) has got an alternative reinforcement in concrete structures due to its excellent corrosion resistance. This study presents a numerical analysis examination of the axial behavior of concrete columns with steel slag as a coarse aggregate partially substitute, and reinforced by locally produced glass fiber reinforced polymer (GFRP) bars as a solution to subdue the corrosion problems, where this material present a relatively modern technique. It is well known steel slag is a by-product material obtained by the melting of steel scrap to mate steel in the electrical arc furnace, recycling steel slag to be usage in the concrete as essential aggregate substitute might show an economical and environment profit. A finite element analysis on 16-column models by using ANSYS ; all modeling were tested in a vertical position and under compressive axial static loading, and all specimens have the same dimensions; 200*200mm cross-section and 1000mm height, main reinforcement of 4Ø12mm, 6Ø12mm, 8Ø12mm, 4Ø16mm, and 4Ø18mm. Transverse reinforcement; Ø6@120mm and Ø6@60mm. The column models with dissimilar parameters (main reinforcement ratios, the main reinforcement types, the transverse reinforcement ratios in the column, and the characteristic strength of concrete) were usage to ponder how dissimilar parameters affect the behavior of reinforced concrete columns by adding 30 % steel slag and reinforced by GFRP bars can be devote in order to get maximum load capacity.

Keywords – Short Columns, Fiber Reinforced Polymer, Steel slag

I. INTRODUCTION

Deterioration of reinforced concrete structures has got a serious proposition in the last decade. This situation is chiefly due to corrosion of steel reinforcing bar embedded in concrete, when exposed to high percent of chlorides and/or sulphates in air, and where salt contaminated aggregates are utilized. Hence, concrete structures bear from corrosion of steel reinforcement; corrosion reduces the reinforcement effective cross section and endangers the uprightness of the structure. Additionally the products of corrosion take up more volume than the original material causing cracking, spalling and delaminating of the concrete cover, which can also put the structure at risk [1]. The rehabilitation or upgrading cost of damaged reinforced concrete members is too much to be neglected, where the estimated repair cost of parking structures is about \$6 billion in Canada [2], over \$50 billion in USA. The cost is \$1 to \$3 trillion for all concrete structures in the USA [3], and about \$3 billion/year in Europe [4]. Excessive corrosion problems also exist in Arabian Gulf countries [5].

Aggregates are the main constituent of concrete, occupying 70% almost of the concrete matrix. In numerous nations there is appropriate of natural aggregate that is suitable for construction whereas in other countries the consuming of aggregate has expanded in later, due to increases in the construction industry. In order to lowers depletion of natural aggregate due to construction, artificially manufactured aggregate and some industrial waste materials can be utilized as alternatives such: (steel slag, silica fumes and Fly ash). Steel slag is a by-product of the steel-making process and the utilization of slag in different contemporary applications is a genuinely later development, Utilizing of steel slag in concrete as a substitution proportion of 15-17.5% by volume for coarse aggregate materials improves the compressive, tensile and flexural strength of concrete, this can manufacturing the high density concrete and has a superior protecting property, with the goal that it can shield from destructive radiations like X-beams, Gamma beams, Neutrons such the atomic structures [6] Steel slag has been utilized in the construction industry as a fractional substitute of either coarse aggregate or fine aggregate. For instance the steel making industries in the U.S. Generate 10-15 million tons of steel slag per year. In 2006, nearly 50 to 70% of the total steel slag produced in the U.S. was utilized as aggregate for road and pavement construction, and the remaining 10 to 15% of the total steel slag generated is utilized in miscellaneous applications. China occupies the first class in the world in production of the steel slag, it generated nearly 740 million tons in 2009, Qatar produce about 500,000 tons of gravel and another

400,000 tons of steel slag yearly [7, 8, &9]. Steel slag is an industrial by-product waste particles resulted from reinforcing steel bars manufacture, its production is very large; total quantity produced from all steel bars manufacture factories in Egypt is about one million tons per year. This slag is currently being utilized in road construction work and utilized as a percentage of coarse aggregates and high density concrete production to utilize in radiation shielding purposes, so researchers began to study the steel slag properties and its impact on the concrete [10]. Khafaga, et al. conducted a study on properties of high density concrete containing steel slag aggregate they tested four groups consisted of 24 normal, high and ultra-high strength concrete mixtures with replacement percentages 0%, 33.33%, 66.67% and 100% by weight of the coarse aggregate with two cement contents (450 kg/m³ and 600 kg/m³). And the results indicated that the highest concrete strength was obtained for the mixtures possessed a percentage of 66.67% steel slag aggregates as a replacement of the coarse aggregate [11]. Qurishee, et al. Investigated the strength properties of slag incorporated with concrete. The extent of stone chips and slag utilized in this examination as coarse total are 0 to 100%. A sum of 500 examples of 4 inches cube was cast, for the periods of 7, 14, 28, 90 and 180 days. W/C ratios were varied as 0.60, 0.50 and 0.42 for making 20, 30 and 40MPa concrete respectively and compressive as well as tensile test were assessed. Concrete made by replacing coarse aggregate is observed to increase up to 40% [12]. Adedokun, et al. studied the utilization of steel slag as replacement for coarse aggregate in concrete. Proved that optimum replacement of coarse aggregate with steel slag that gives better mechanical properties (compressive strength, tensile strength and flexural strength) than conventional concrete is found to be between 30 and 60% [13]. Safdar, et al. studied the analytically on "application of steel slag as fractional additional of coarse aggregates" replacement of natural coarse aggregates by different ratio of steel slag at 20, 40, 60, 80 and 100% by using the mix design of concrete and its strength was more than 4500 psi. [14]. Hadi, et al. had carried a study on 12 circular concrete specimens with 205 mm diameter and 800 mm height, under different loading cases. The samples were reinforced with normal steel bars and spirals, GFRP bars, and different of GFRP spirals, and results shown the spacing of the cracks in the steel-RC specimens was about 60 mm, which was approximately 6.3% smaller than the crack spacing of the corresponding GFRP-RC specimens. The spacing of the cracks in the specimens with 30-mm pitch of the GFRP helix (about 54 mm) was about 15.6% smaller than the specimens with 60-mm pitch of the GFRP helix (about 64 mm). -The contribution of the steel bars was nearly two times more than the contribution of the longitudinal GFRP bars (around 13.4%). Reducing the spacing of the GFRP helices from 60 to 30 mm led to and grows in the first peak load and ductility by around 7 and 29%, respectively [15]. Fillmore, et al. studied contribution of Longitudinal GFRP Bars in Concrete Cylinders under Axial Compression by testing 21 concrete cylinders (150 mm×300 mm) reinforced with longitudinal GFRP and steel bars in compression, the inference of showed that the elastic modulus of GFRP bars in compression is marginally higher than that of in tension, however the compressive strength was get 67% of tensile strength. The load capacity of the specimens was within 4.5-18.4% relative to the bars reinforcement ratio renormalize to the elastic modulus of steel bars [16]. Al-Ajarmeh, et al. studied the axial behavior of hollow concrete columns reinforced with glass-fiber-reinforced-polymer (GFRP) bars and spirals with different inner-to-outer diameter ratios. used four concrete columns 250 mm in external diameter and reinforced longitudinally with six 15.9 mm diameter GFRP bars were cast with different inner diameters (0, 40, 65, and 90 mm) and tested under concentric axial loading. The results proved the hollow concrete columns reinforced with GFRP bars and spirals exhibited 11% higher axial capacity than the steel reinforced hollow column. The GFRP-reinforced hollow columns showed 22% and 54% higher ductility and confinement efficiency, respectively [17]. Recycling steel slag to utilize it in the concrete as natural aggregate replacement might prove an economical and environmentally friendly solution also this will encourage other investigations to find another filed of using the slag. As a substitute to steel reinforcement, Fiber Reinforced Polymers (FRP) bars have suitable inferiority due to their noncorrosive and non-metallic properties. FRP are light weight and have high strength-to-weight ratios 1.5 to 2 times the tensile strength of steel. Glass fiber reinforced polymer GFRP has a very significant role to act as reinforcement in concrete structures that will be exposed to severe environmental conditions where traditional steel reinforcement could corrode. FRP is the most corrosion resistance replacement of steel reinforcement in concrete, the corrosion reduces the life time of structures, causes high repair costs. With this combination between a by-product aggregate and non- corrosion reinforcement we can offer a cost effective reinforced concrete section that can achieve very high compression and very high durability against corrosion if we compare with normal concrete section reinforced with steel bars.

II. OBJECTIVE OF THE STUDY

The main objectives of this study could be summarized in the following points

- To investigate the general behavior of RC columns by adding steel slag and reinforced longitudinally with GFRP bars under axial loads.

- To determine the ultimate loads of RC columns with adding steel slag and reinforced with GFRP bars, steel stirrups.
- To determine the ultimate vertical displacement and ultimate lateral displacement of RC columns with adding steel slag and reinforced with GFRP bars.

To evaluate and interpretation of test data with detailing parameters..

III. NUMERICAL STUDY

The objective of this paper is to study the behavior of reinforced concrete columns with steel slag as a portion of coarse aggregate reinforced with FRP and steel bars using finite element models by ANSYS. The studied parameters include (main reinforcement ratios, the main reinforcement types, the transverse reinforcement ratios in the column, and the characteristic strength of concrete). Hence, compared results with experimental results as described and predict a general formula to design.

3.1. Finite element columns modeling

3.1.1. Geometry of specimens

Analysis is carried out on 16- columns models, divided into six groups as shown in table 1, all columns are square cross-section with a 200 mm side and length of 1000 mm. The main reinforcement is GFRP bars 4Ø12 mm, 6Ø12 mm, 8Ø12, 4Ø16 and 4Ø18 mm and steel bars 4Ø12 mm. The transverse reinforcement was Ø6 mm closed stirrups spread in 120 mm, and 60 mm, and characteristic strength of concrete columns is 25,30, 35,40 ,45 N/mm². All columns were subject to vertical load on top surface and ideal bond between concrete and the reinforced bars is assumed. Figure (1) shows details of columns reinforcement models.

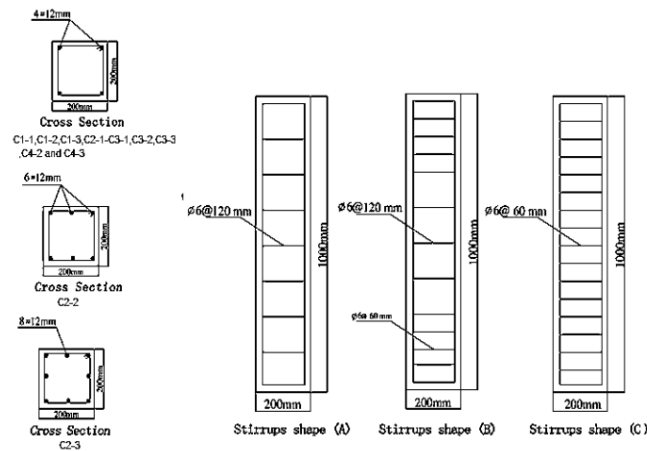


Figure (1): Details of columns reinforcement models

Table (1): Detail sand reinforcement of columns models for groups 1,2,3,4,5&6

G. No.	Col. No	Steel slag %	f_{cu} (N/mm ²)	Reinf.	Bar type	ρ_s %	Stirrups
1	C1-1	0	30	4Ø12mm	Steel	1.131	Ø6mm @ 120mm-Shape(A)
	C1-2	0			GFRP		
	C1-3	30			GFRP		
2	C2-1	30	30	4Ø12mm	GFRP	1.131	Ø6mm @ 120mm- Shape(A)
	C2-2			6Ø12mm		1.698	
	C2-3			8Ø12mm		2.263	
3	C3-1	30	30	4Ø12mm	GFRP	1.131	Ø6mm @ 120mm - Shape(A)
	C3-2						Ø6mm @ 60mm-Shape(B)
	C3-3						Ø6mm @ 60mm-Shape(C)
4	C4-1	30	30	4Ø12mm	GFRP	1.131	Ø6mm @ 120mm-Shape(A)
	C4-2		35				
	C4-3		40				
5	C5-1	30	30	4Ø16mm	GFRP	2.011	Ø6mm @ 120mm-Shape(A)
	C5-2		4Ø18mm	2.546			
6	C6-1	30	25	4Ø12mm	GFRP	1.131	Ø6mm @ 120mm-Shape(A)
	C6-2		45	4Ø12mm			

3.2. Element types

3.2.1 Concrete element

The concrete was modeled using 8 node solid element labeled by Solid65 in ANSYS. Solid65 is utilized for the 3-D modeling of solids with or without reinforcing bars (rebar). The solid element has eight nodes with three degrees of freedom at each node. The element is proficient of plastic deformation, cracking in three orthogonal directions, and crushing. The most important aspect of this element is the treatment of nonlinear material properties. The concrete is proficient of cracking (in three orthogonal directions), crushing, plastic deformation, and creep. They are also proficient of plastic deformation and creep. The geometry, node locations, and the coordinate system for this element are shown in figure (2). The uniaxial concrete compressive strength of each column is presented by. The Young modulus, uniaxial tensile strength, and Poisson ratio are assigned to $4400\sqrt{f_{cu}}$ N/mm², $0.6\sqrt{f_{cu}}$ N/mm², and 0.2 respectively.

3.2.2 Reinforcement element

A link180 element was utilized to model the reinforcement polymer bar and steel; two nodes are required for this element. Each node has three degrees of freedom, translation in the nodal x, y, and z directions. The element is also capable of plastic deformation; LINK180 -3-D bar is shown in figure (3).

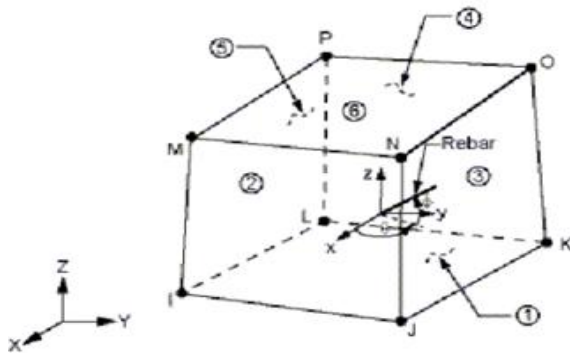


Figure (2): SOLID65 geometry, node locations, and the coordinate system

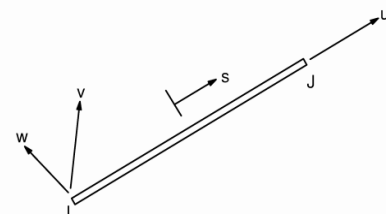


Figure (3): LINK180 -3- D bar

3.2.3 Collar plates element

A Solid185 element was utilized for steel plates in the encirclement of concrete columns at the ends. This element is utilized for the 3-D modeling of solid structures and has eight nodes with three degrees of freedom at each node – translations in the nodal x, y, and z directions. The geometry and node locations for this element are shown in figure (4).

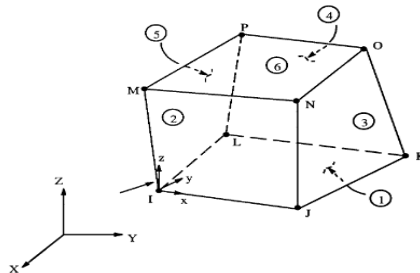


Figure (4): SOLID 185 -3-D solid

3.3. Material properties

3.3.1 Concrete

Development of a model for the behavior of concrete is a challenging task. Concrete is a quasi-brittle material and has different behavior in compression and tension. The tensile strength of concrete is typically 8-15% of the compressive strength. Figure (5) shows a typical stress-strain curve for normal weight concrete.

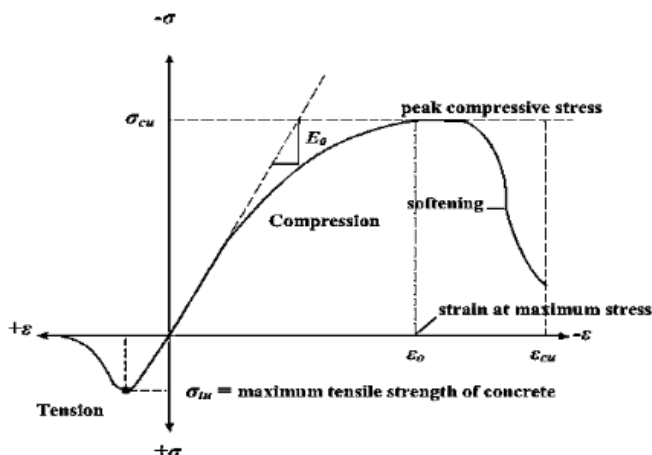


Figure (5): Typical uniaxial compressive and tensile stress-strain curve for concrete

In compression, the stress-strain curve for concrete is linearly elastic up to about 30% of the maximum compressive strength. Above this point, the stress increases up to the maximum compressive strength. After it reaches the maximum compressive strength σ_{cu} , the curve descends into a softening region, and eventually crushing failure occurs at an ultimate strain ϵ_{cu} . In tension, the stress-strain curve for concrete is linearly elastic up to the maximum tensile strength. After this point, the concrete cracks and the strength decreases to zero. The input data for the concrete, GFRP, and steel bars properties are shown in tables (2). Figures (6 &7) show a stress-strain curve for steel reinforcement and stress-strain curves for the FRP composites in the direction of the fibers respectively.

Table (2): Summary data for specimen materials

Item	Type of Element	Material number	Model	Real constant number
Concrete	SOLID 65	1		1
Longitudinal steel bars	LINK 180	2		2
Longitudinal GFRP bars	LINK 180	3		3
Transverse bars	LINK 180	4		3
Steel plates	SOLID 185	5		-

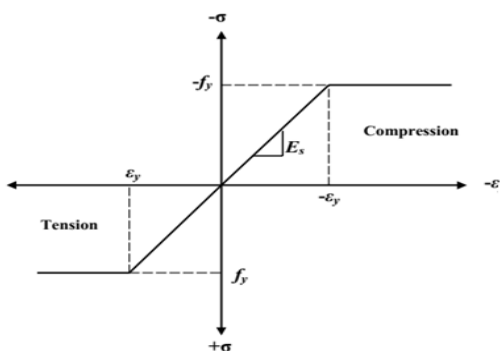


Figure (6): Stress-strain curve for steel reinforcement

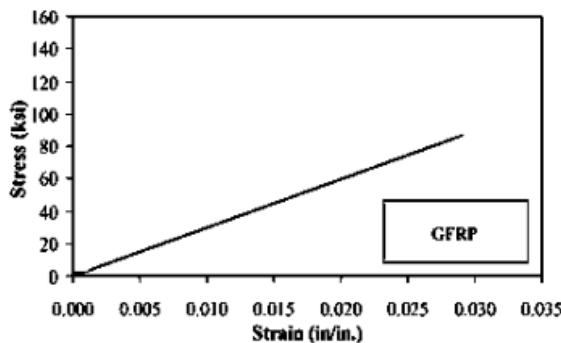


Figure (7): Stress-strain curve for the GFRP composites in the direction of the fibers

3.4. Modeling

The concrete column, reinforcement bars, and collar plates the main components of the model. The model is 1000 mm long, with a cross-section of 200 mm width and 200 mm depth. Two steel plates of 200mm width and 200mm height and 6mm thickness are modeled to support the concrete columns at the ends, as shown in figure(8). The combined volumes of the plate and column are shown in figure (9). Link180 element is utilized to create the compression and shear reinforcement as shown in figure (10). The Combined volumes of the reinforcement and Column are shown in figure (11).

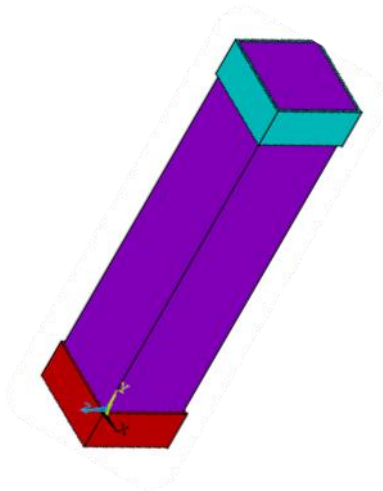


Figure (8): Combined volumes of the plate and column

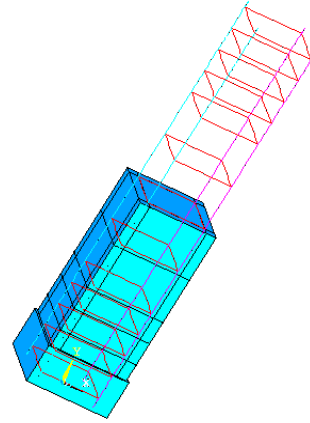


Figure (9): Combined volumes of the reinforcement, concrete and plates

3.5. Meshing

The mesh sizing command was utilized to mesh all elements. To obtain good results from the Solid65 element, the utilization of a rectangular mesh is recommended. Therefore, the mesh was set up such that square elements with 25 mm length, Ø6 stirrups bars reinforcement located 25mm from the end of the Cross-Section Shared nodes of stirrups and rebar #12 bar reinforcement. The mesh generated as shown in figure (11). Mesh of the concrete ,steel plate and bars are shown in figure (10).

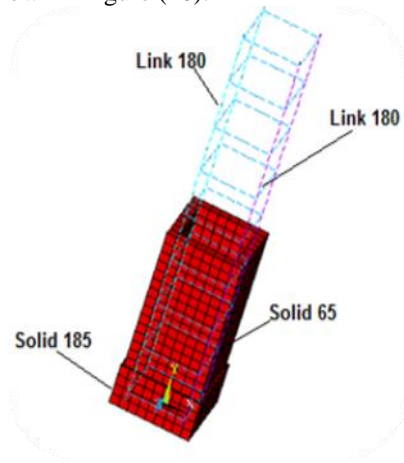


Figure (10): Mesh of the concrete ,steel plate and bars

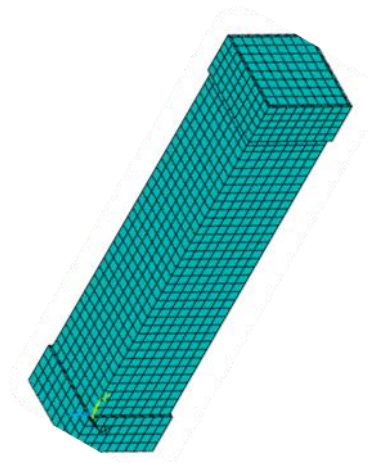


Figure (11): Finite element mesh for column model

3.6. Loading

A nonlinear structural analysis was performed to study the nonlinear behavior of RC columns. In nonlinear analysis, applied load to a finite element model is divided into a series of load increments called load step, at the completion of each load increment the ANSYS program utilizes Newton-Raphson equilibrium iterations for updating the model stiffness. The simplified stress- strain curve for model is constructed from 6 points connected by straight lines as shown in figure (12).

3.7. Boundary conditions and loads

The boundary conditions were chosen to simulate the experimental conditions. The horizontal translations of all base joints were restrained in the three directions. Figure (13) shows the boundary conditions and figure (14) shows the method of loading of specimen.

$$f = \frac{E_c \epsilon}{1 + \left(\frac{\epsilon}{\epsilon_0}\right)^2} \quad (1)$$

$$\epsilon_0 = \frac{2f'_c}{E_c} \tag{2}$$

$$E_c = \frac{f}{\epsilon} \tag{3}$$

Where:

f = stress at any strain ϵ psi

ϵ = strain at stress f

ϵ_0 = strain at the ultimate compressive strength f'_c

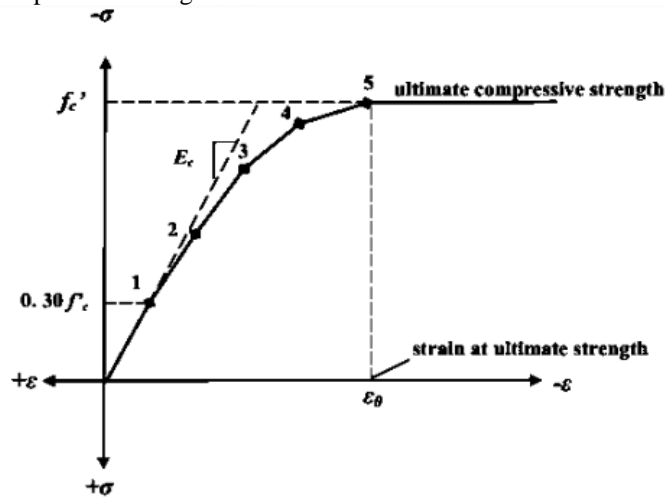


Figure (12): Simplified compressive axial stress-strain curve for concrete

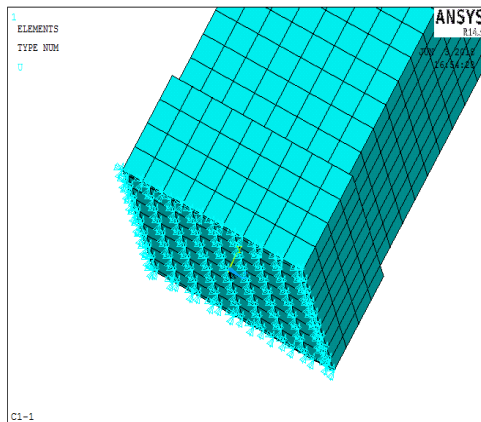


Figure (13): Boundary conditions

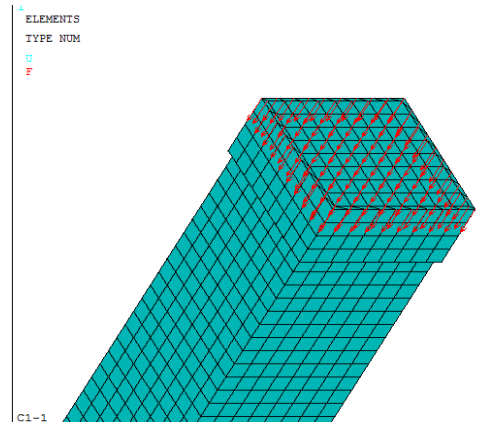


Figure (14): Specimen loading

IV. RESULTS

The results of the numerical analysis of column models are shown in table (3), table includes the values of the maximum loads (Pmax), maximum vertical displacement δ_v (mm), maximum horizontal displacement δ_h (mm), initial cracking loads (Pcr) and Toughness of tested modeling.

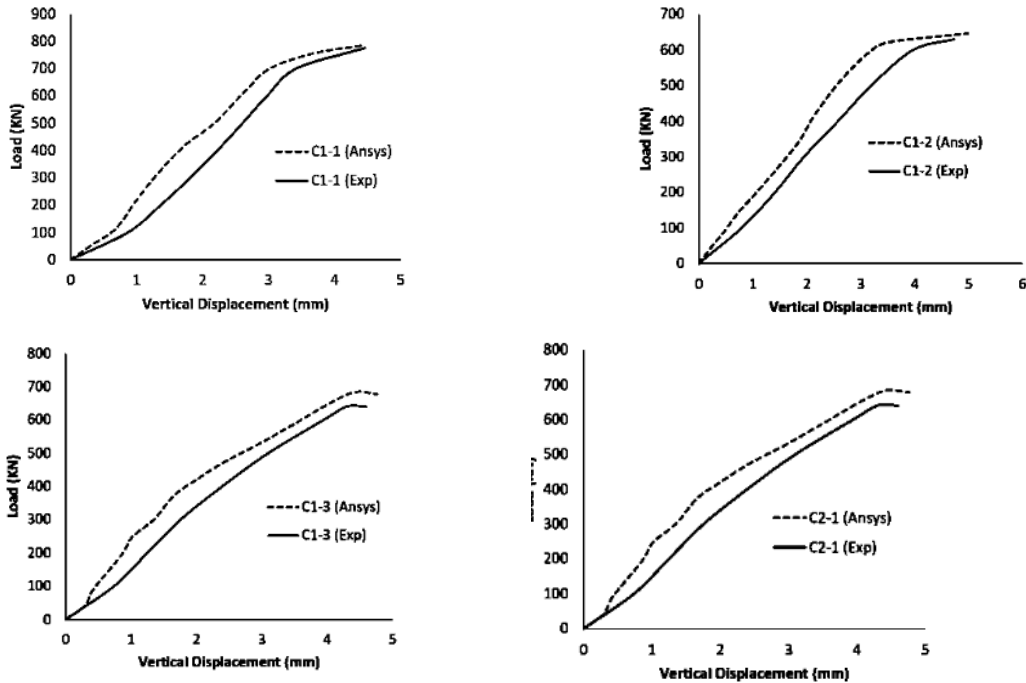
Table (3): Numerical results of tested columns specimens

Col.	Group No.	f_{cu} (N/mm ²)	P_{cr} (KN)	P_{max} (KN)	Max vertical displacement δ_v (mm)	Max horizontal displacement δ_h (mm)	Toughness (KN.mm)
C1-1	1	30	424	800	4.540	0.201	1899
C1-2			441	646	4.980	0.351	1726
C1-3			450	678	4.760	0.253	1703
C2-1	2	30	450	678	4.760	0.253	1703
C2-2			344	720	5.600	0.301	1890
C2-3			501	815	3.600	0.511	2385
C3-1	3	30	450	678	4.760	0.253	1678
C3-2			435	727	4.300	0.657	2023
C3-3			450	850	4.580	0.728	2671
C4-1	4	30	450	678	4.760	0.253	1684
C4-2		35	460	930	5.100	0.541	2470
C4-3		40	492	1190	5.190	0.406	2955
C5-1	5	30	356	778.3	3.801	0.614	2043
C5-2			433	903.4	3.75	0.488	2385
C6-1	6	25	327	559.7	3.951	0.198	901
C6-2		45	468	1350	6.027	0.526	3196

V. ANALYSIS AND DISCUSSION

5.1 Experimental Validation

The validity of the proposed numerical model is checked through extensive comparisons between numerical and experimental results of RC columns under compression load [18]. Figure 15 shows the numerical and experimental load-deformation curves of tested specimens. The numerical results from finite element analysis showed in general a good agreement with the experimental values.



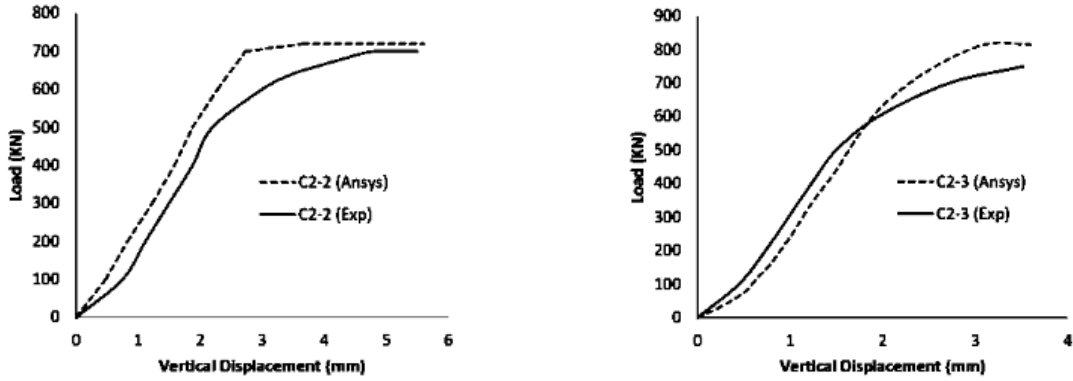
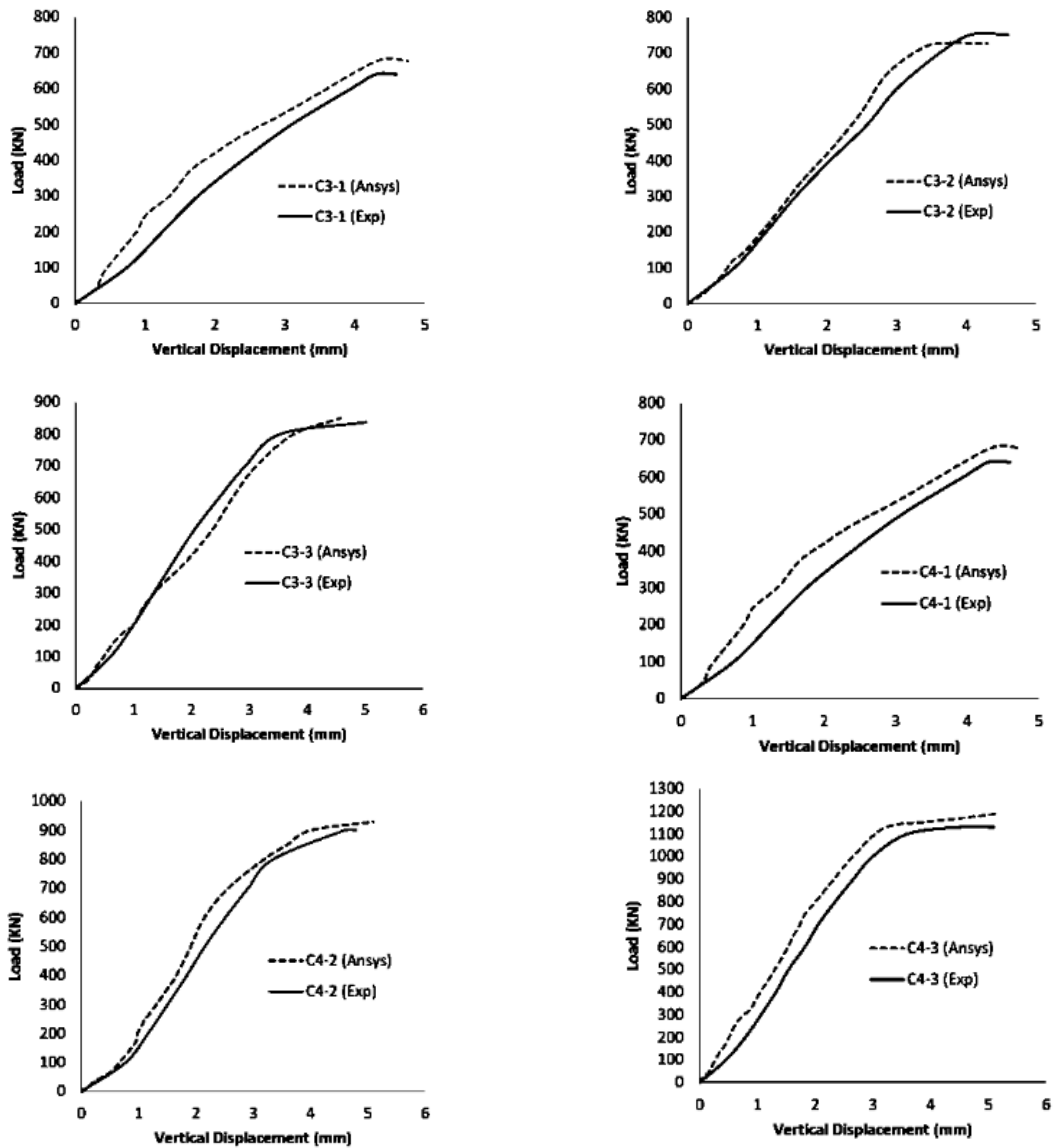


Figure (15): Load– Vertical displacement relationship obtained from both experimental and numerical result



Cont. Figure (15): Load– Vertical displacement relationship obtained from both experimental and numerical result

5.2 The main reinforcement ratios

Figure (16) shows the load- vertical displacement of columns C2-2, C5-1, C5-2, C2-3 and C2-1 which reinforced by GFRP reinforcement ratio; 1.698, 2.011, 2.263 and 1.131%. Ultimate load, initial cracking loads and toughness of tested columns C2-2, C5-1, C5-2, C2-3 to C2-1 are (106, 76, 111%), (115, 79, 127%), (120, 111, 132%) and (133, 96, 140%) respectively.

Figure (17) shows the effect of the main reinforcement ratios on the ultimate load that the columns resists, where the increasing of main reinforcement ratios has a significant effect on ultimate loads, after reinforcement ratio 2.011%

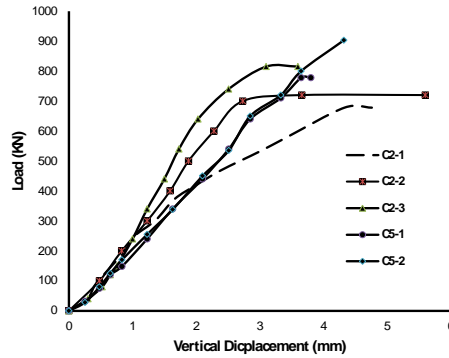


Figure (16): Load – Vertical displacement relationship for models with different reinforcement ratios

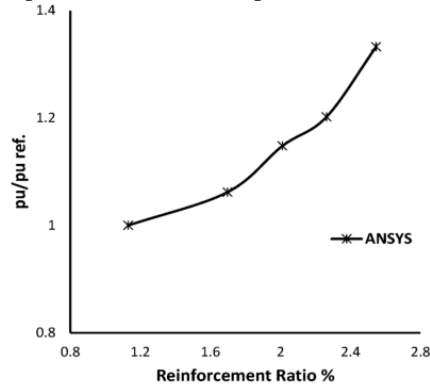


Figure (17): main reinforcement ratios on the ultimate load

5.3 The main reinforcement types

Figure (18) shows the load- vertical displacement of columns C1-2; reinforced by GFRP bars and 0% steel slag, C1-3; reinforced by GFRP bars and 30% steel slag and C1-1; reinforced by steel bars and 0% steel slag. Ultimate load, initial cracking loads and toughness of tested columns C1-2, C1-3, to C1-1 are (80, 104, 91 %), and (85, 106, 90%) respectively.

Using main reinforcement of GFRP bars increase the horizontal and vertical strain where reduce ultimate loads, and toughness of tested columns.

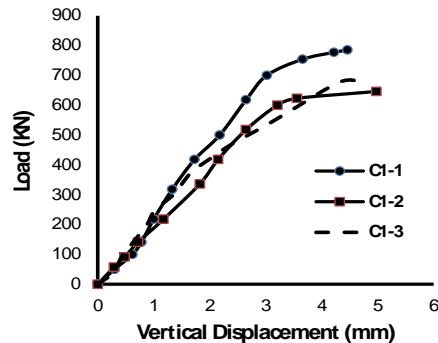


Figure (18): Load – Vertical displacement relationship for finite element models C1-1, C1-2 and C1-3

5.4 The transverse reinforcement ratios in the column

Figure (19) shows the load- vertical displacement of columns C3-2, C3-3, and C3-1 which have different stirrups distribution B, C and A respectively. Ultimate load, initial cracking loads and toughness of tested columns C3-2, C3-3 to C3-1 are (107, 90, 121%), and (125, 96, 159%), respectively.

Increasing transverse reinforcement ratios in the column with GFRP bars has a significant effect on ultimate loads and toughness of tested columns, where increasing of transverse reinforcement ratios confines the columns so it is lead to increase the ultimate loads and toughness which the columns resisted.

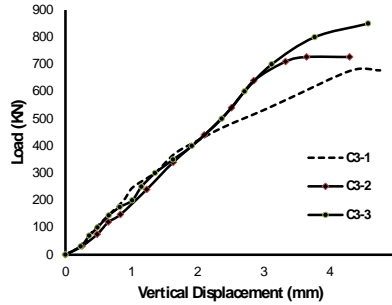


Figure (19): Load – Vertical displacement relationship for finite element models with different transverse reinforcement ratios

5.5 The characteristic strength of concrete

Figure (20) shows the load- vertical displacement of columns C4-1, C4-2, C4-3, C6-2 and C6-1 which have characteristic strength of concrete 30, 35, 40, 45 and 25 N/mm². Ultimate load, initial cracking loads and toughness of tested columns C4-1, C4-2, C4-3, C6-2 and C6-1 are (121, 138, 187%), (166, 141, 274%), (212, 150, 328%) and (241, 143, 355%) respectively.

Figure (21) shows the effect of the characteristic strength of concrete on the ultimate load that the columns resists, where the increasing of characteristic strength of concrete has a significant effect on ultimate loads.

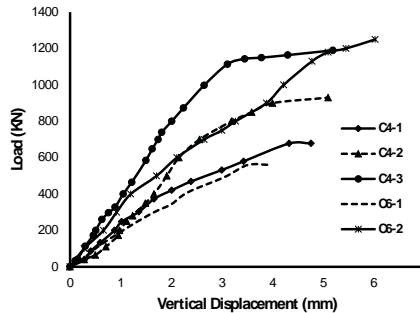


Figure (20): Load – Vertical displacement relationship for finite element models with different characteristic strength of concrete

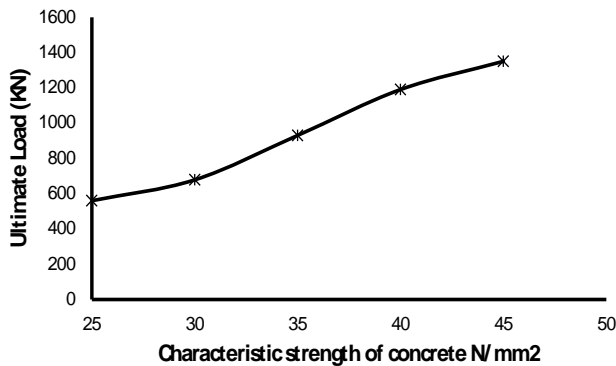


Figure (21): Ultimate load and characteristic strength of concrete.

VI. PREDICTED DESIGN FORMULA

The calculation of the ultimate load through the Egyptian, American and British codes by the equations for the design of the concrete columns on all the specimens and comparing them with numerical and experimental results as shows in table (4).

Table (4): Ultimate loads and vertical displacement for all models by different cods.

G. No.	Col.	Reinf. Ratio %	F _{cu} (KN)	Ultimate loads P _u (KN)					Ultimate Vertical Dis. δ (mm)		$\frac{\delta_{EXP}}{\delta_{F.E.}}$
				Exp.	Finite element (ANSYS)	(ACI:318) ¹	(BSI: 8110) ²	(ECP: Code) ³	Exp.	Finite element (ANSYS)	
1	C1-1	1.131	30	774	800	698	755	572	4.455	4.540	0.981
	C1-2	1.131	30	630	646	696	751	569	4.713	4.980	0.946
	C1-3	1.131	30	640	678	665	722	546	4.300	4.760	0.903
2	C2-1	1.131	30	640	678	665	722	546	4.300	4.760	0.903
	C2-2	1.698	30	680	720	727	828	621	9.500	5.60	1.696
	C2-3	2.263	30	724.5	815	789	933	695	3.520	3.60	0.977
3	C3-1	1.131	30	640	678	665	722	546	4.300	4.760	0.903
	C3-2	1.131	30	758.1	727	818	981	729	5.810	4.30	1.351
	C3-3	1.131	30	837.33	850	889	1102	814	4.084	4.580	0.891
4	C4-1	1.131	30	640	678	665	722	546	4.300	4.760	0.903
	C4-2	1.131	35	1011.4	930	905	949	723	3.196	5.100	0.626
	C4-3	1.131	40	1137.6	1190	987	1026	7863	5.016	5.190	0.966
5	C5-1	2.011	30	-	778.3	766	893	667	-	3.801	-
	C5-2	2.56	30	-	903.4	834	1008	748	-	4.321	-
6	C6-1	1.131	25	-	559.7	600	661	499	-	3.511	-
	C6-2	1.131	45	-	1250	1038	1075	821	-	6.027	-

1-American Concrete Institute, Committee ACI 440.1 R-06 [19].

2- British Standards Institution (BS 8110-1 1997) [20].

3- Egyptian Code of Practice for design and construction requirement of using fiber reinforced polymers in construction field ECP (208-2007) [21].

Figure (22) shows the effect of the main reinforcement ratios on the ultimate load; hence a new general formula was predicted from the experimental data, which was the average of data, as following:

$$P_u = 0.41 f_{cu} A_c + 0.73 f_y A_s$$

P_u : Ultimate axial load of the reinforced concrete column with GFRP.

f_{cu} : Characteristic of concrete by adding 30% steel slag.

A_c : Area of concrete cross-section.

f_y : Characteristic of reinforcement GFRP bars.

A_s : Area of reinforcement cross-section

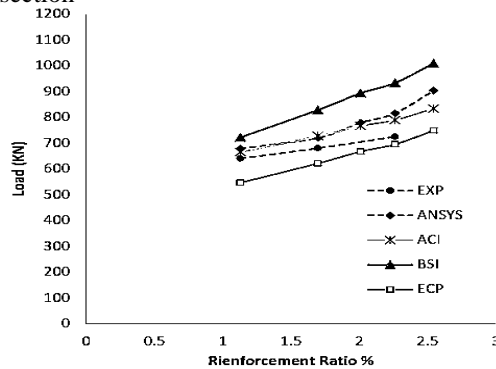


Figure (22): Relation between ultimate load and reinforcement ratios

VII. CONCLUSIONS

This study investigated the flexural behavior of concrete beams with steel slag as a coarse aggregate replacement reinforced by locally produced glass fiber reinforced polymer (GFRP) bars. Within the scope of the experimental

program considering the materials utilized, comparison of the experimental results with the values calculated using the calibration model and other numerical models resulted in the following conclusions:

- Using steel slag as a coarse aggregate replacement with reinforced by GFRP bars might prove an appropriate solution for short columns
- Increasing of main reinforcement ratios; 1.131 to 2.546% with 30% steel slag increases ultimate loads of tested columns from 106 to 133%.
- Increasing of main reinforcement ratios with 30% steel slag has a significant effect on ultimate loads, after reinforcement ratio 2.011%.
- Using main reinforcement of GFRP bars and 30% steel slag increase the horizontal and vertical strain where reduce ultimate loads, and toughness of tested columns.
- Increasing transverse reinforcement ratios in the column with GFRP bars and 30% steel slag increase ultimate loads; from 107 to 125% and toughness of tested columns; from 121 to 159%.
- Increasing of characteristic strength of concrete; 25, 30, 35, 40, and 45 N/mm² has a increase ultimate loads of tested columns with GFRP bars and adding 30% steel slag from 121 to 241%.
- A new general formula was predicted for design of columns with GFRP and 30% steel slag as a coarse aggregate partially replacement:

$$P_u = 0.41 f_{cu} A_c + 0.73 f_y A_s$$

P_u : Ultimate axial load of the reinforced concrete column with GFRP.

f_{cu} : Characteristic of concrete by adding 30% steel slag.

A_c : Area of concrete cross-section.

f_y : Characteristic of reinforcement GFRP bars.

A_s : Area of reinforcement cross-section

VIII. REFERENCES

- [1] Hanus J. P., Shield C. K. and French C. W., "Development Length of GFRP reinforcement in Concrete Bridge Decks" Final Report Prepared, July 2000, Published by Minnesota Department of Transportation.
- [2] Chaallal O. and Benmokrane B., "Fiber-reinforced plastic rebars for concrete applications", Composites, Part B 27B (1996), 245-252 pp Copyright! 1996 Elsevier Science Limited, Printed in Great Britain.
- [3] Fickelhorn M., "Eiditorial" Materials and structures journal, RILEM, Vol.23, No. 137, 1990, pp 317.
- [4] Clark J. L., "The need for durable reinforcement" Alternative Materials for the reinforcement and prestressing of concrete, J. L. Clark, ed., 1993, pp.1-33.
- [5] Makhtouf H. M., Abmadi B. H., and Al-Jabal J., "Preventing reinforced concrete deterioration in Arabian Gulf "Concrete International, Vol. 13, No. 5, May 1991, pp. 65-67.
- [6] Yu, X. "Concrete made with steel slag and waste glass and its application in concrete-filled steel tubular columns". Doctoral dissertation, Western Sydney University (Australia), 2017.
- [7] Yildirim, I. Z., & Prezzi, M. (2009). "Use of steel slag in subgrade applications". Publication FHWA/IN/JTRP-2009/32. Joint Transportation Research Program, Indiana Department of Transportation and Purdue University, West Lafayette, Indiana.
- [8] Chunlin, L., Kunpeng, Z., & Depeng, C. (2011). "Possibility of concrete prepared with steel slag as fine and coarse aggregates: A preliminary study". Procedia Engineering, 24, 412-416.
- [9] Taha, R., Sirin, O., & Sadek, H. (2014). "Recycling of Local Qatar's Steel Slag and Gravel Deposits in Road Construction". International Journal of Waste Resources, ISSN:2252-5211 IJWR, Volume 4 . Issue 4 .1000167.
- [10] Zaki, S. I., Metwally, I. M., & El-Betar, S. A. (2011). "Flexural Behavior of Reinforced High-Performance Concrete Beams Made with Steel Slag Coarse Aggregate". ISRN Civil Engineering, 2011.
- [11] Khafaga, M. A., Fahmy, W. S., Sherif, M. A., & Hamid, A. A. (2014). "Properties of high strength concrete containing electric arc furnace steel slags aggregate". Journal of Engineering sciences, Assiut University, Egypt, 42(3), 582-608.
- [12] Qurishee, M. A., Iqbal, I. T., Islam, M. S., & Islam, M. M. (2016). "Use of slag as coarse aggregate and its effect on mechanical properties of concrete". In Proceedings of 3rd International Conference on Advances in Civil Engineering.
- [13] Adedokun, S. I., Anifowose, M. A., & Odeyemi, S. O. (2018). "ASSESSMENT OF STEEL SLAG AS REPLACEMENT FOR COARSE AGGREGATE IN CONCRETE: A REVIEW". Acta Technica Corviniensis-Bulletin of Engineering, 11(4), 139-146.
- [14] Safdar, M. A., Mohammad, M., Ahmad, S., & Shah, S. W. A. (2019). "Application of by Product of a Steel (Steel Slag) As Fractional Additional of Mixture Coarse Aggregate in Concrete". Advances in Social Sciences Research Journal, 6 (2).
- [15] Hadi, M. N., Karim, H., & Sheikh, M. N. (2016). "Experimental investigations on circular concrete columns reinforced with GFRP bars and helices under different loading conditions". Journal of Composites for Construction, 20(4), 04016009.
- [16] Fillmore, B., & Sadeghian, P. (2018). "Contribution of longitudinal glass fiber-reinforced polymer bars in concrete cylinders under axial compression". Canadian Journal of Civil Engineering, 45(6), 458-468.
- [17] AlAjarmeh, O. S., Manalo, A. C., Benmokrane, B., Karunasena, W., Mendis, P., & Nguyen, K. T. Q. (2019). "Compressive behavior of axially loaded circular hollow concrete columns reinforced with GFRP bars and spirals". Construction and Building Materials, 194, 12-23.
- [18] Aljabri, Q. M., (2019). "BEHAVIOR OF REINFORCED CONCRETE COLUMNS BY USING STEEL SLAG AND REINFORCED BY FRP GLASS BARS." Department of Civil Engineering, Faculty of Engineering, SUEZ CANAL UNIVERSITY
- [19] ACI (American Concrete Institute). (2015). "Guide for the design and construction of structural concrete reinforced with FRP bars". ACI 440.1 R-06.
- [20] British Standards Institution (BS 8110-1 1997) "Structural use of concrete — Part 1: Code of practice for design and construction"
- [21] Egyptian Code of Practice for design and construction requirement of using fiber reinforced polymers in construction field ECP (208-2007).